

Compressive Strength and Bonding Performance of Concrete Beams Strengthened with GFRP Plates

Ahmad Kamil Aminuddin¹, Sakhiah Abdul Kudus^{1,2}, Nurul Ain Nafisa Kasmizi¹, Mohamad Farid Misnan^{3,4*}, Sharifah Salwa Mohd Zuki⁵, Mohamad Azim Mohammad Azmi⁶, Shahiron Shahidan⁵

¹ Faculty of Civil Engineering,

Universiti Teknologi MARA, 40450 Shah Alam, Selangor, MALAYSIA

² Institute for Infrastructure Engineering and Sustainable Management (IIESM), Universiti Teknologi MARA, (UiTM), Shah Alam, Selangor, MALAYSIA

³ Faculty of Electrical Engineering,

Universiti Teknologi MARA, 40450 Shah Alam, Selangor, MALAYSIA

⁴ Smart Manufacturing Research Institute (SMRI)

Universiti Teknologi MARA, (UiTM), Shah Alam, Selangor, MALAYSIA

⁵ Faculty of Civil Engineering and Built Environment,

Universiti Tun Hussein Onn Malaysia, Parit Raja, 86400 Batu Pahat, Johor, MALAYSIA

⁶ Center for Diploma Studies, Universiti Tun Hussein Onn Malaysia,

Education Hub Pagoh, 84600 Muar, Johor, MALAYSIA

*Corresponding Author: mohamadfarid@uitm.edu.my

DOI: <https://doi.org/10.30880/ijie.2025.17.05.024>

Article Info

Received: 29 August 2024

Accepted: 10 April 2025

Available online: 30 August 2025

Keywords

GFRP plate, concrete degradation, structural performance, bonding performance, flexural capacity, repair methods

Abstract

This study aims to test the bond strength and the structural response of concrete beams reinforced with Glass Fiber Reinforced Polymer (GFRP) plates. The experimental program included a total of 41 prisms, of which 12 were tested for compressive strength, and 25 were configured into beams with four-point loading systems, referred to as the GFRP beam set. In total, six beams attached GFRP plates of 50 mm x 100mm and 200 mm (GFRPP-50 and GFRPP-100), while three beams served as control specimens without externally bonded plates. The findings verified that when GFRPP-100 was used as reinforcement, its ultimate load-bearing capacity increased by 137% compared to the controls, being substantially stronger than the other beams. The research emphasizes the role of the epoxy adhesives described in the methods section, including the bonding surface preparation, enabling a cohesive bond connection. GFRP confinement may be used as an innovative strengthening method instead of traditional methods which results in improved structural performance. Further investigations should look into the effects of differing environmental exposures and durations of loads applied on the durability of GFRP-reinforced beams over time. This study provides evidence to facilitate the acceptance of GFRP as an efficient reinforcement tool that improves the serviceability lifespan.

1. Introduction

Concrete continues to be the most popular construction material because of its reasonably priced, multifunctional, and structurally sound properties. Nonetheless, it is often subject to various aging processes, such as cracking, spalling, and scaling, which compromise durability and structural integrity [1], [2]. A notable constituent, cracking, is caused by thermal expansion and shrinkage or overloading, which facilitates the infiltration of moisture and chlorides, aggravating additional distress [3]. Like spalling, cracking also results from the expansion of corroded steel reinforcement coupled with alkali-aggregate reactions and freeze-thaw cycles, resulting in material loss and diminished load capacity [4], [5]. Scaling causes the surface to lose its integrity while exposing inside components. [6] define the condition as faulty finishing methods, repetitive use of deicing salts, and exposure to severe weather. Though traditional methods of mitigation, including epoxy injections and epoxy repairs, offer some relief, they have a host of other issues, such as high costs and further corrosion [7], [8]. Because of the difficulties mentioned before, researchers have sought other materials to enhance its durability and long-term performance.

The advantages of GFRP-reinforced concrete structures have been recognized in marine and bridge construction because they require less maintenance and are less prone to environmental damage over time while providing better results compared to other materials. It is particularly accurate given that the components are not prone to corrosion [9], [10]. Moreover, it has been found that GFRP-reinforced beams provided greater durability and load-bearing capacity compared to their steel-reinforced counterparts, which is key for the problem of structural aging [11]–[13]. Other studies also noted that using GFRP bars instead of steel reinforcement considerably improves long-term performance in structures exposed to wet and chloride-rich environments [14] – [15]. Nevertheless, these benefits require further scrutiny of the effects of changing loads and environmental conditions on the long-term behavior of GFRP.

Beyond GFRP, some studies have focused on the strengthening of concrete beams using steel plates as an alternative. Abdullah et al. [16] carried out an experimental investigation on reinforced concrete beams strengthened with steel plates externally, evaluating various techniques for adhesive placement. The results showed that Sikadur 31 epoxy adhesive led to significantly improved flexural strength in bonded beams, with one specimen showing a 147% increase in load compared to the control beam. While these results illustrate the benefits of epoxy bonds in structural reinforcement, they remind us that optimizing adhesive characteristics to improve performance remains a key challenge. If epoxy bonding improves the strength of the steel plates, the same methods could be applied to increase the effectiveness of GFRP plate reinforcement. Determining the best approach for bonding GFRP to plain concrete beams, however, is still a challenge that needs to be addressed.

The bonding behavior between GFRP and concrete is very important for supporting structures because it affects both the flexural strength and the durability over time. The bond joint must be sufficiently strong to optimize load transfer and the stability of the structure with GFRP-reinforced concrete. Several studies show that aspects like surface preparation, choice of glue, and even the surrounding environment have a great influence on bond strength and failure modes [17], [18]. For example, Bui [17] showed that the composite's adhesive constituents influence interfacial bond stiffness and segment fracture energy, which, to a great extent, governs shear strength in GFRP-strengthened beams. In addition, as Rageh et al. [18] pointed out that surface treatments are necessary for achieving an increase in the strength of adhesion as well as mechanically interlocking with concrete, thus enhancing structural efficiency.

Besides increasing the risk of failure in the bonding performance of GFRP, high chloride exposure and moisture levels can complicate bonding performance even further. For environments where it is repetitively used, such as in bridges and marine structures, deep studies are required to evaluate the strength longevity. Studies also show that GFRP commonly withstands heavy conditions, but with improper bond design, the structure succumbs to external forces and suffers damage through softening, warping, and cracking [19], [20]. Studies emphasize the need to choose the right adhesive and optimize bonding to lessen the risk of degradation and increase performance overall [21].

GFRP not only adds immense damping efficiencies in bonding but also enhances GFRP's flexural performance in concrete beams. It increases resistance to bending and deformation under load. GFRP is better than traditional steel reinforcement in concrete constructions because of its high tensile strength and stiffness [22]. While GFRP is still helpful, research indicates that GFRP-reinforced beams surpass in flexural performance, but under certain conditions, the overall strength is lower than steel-reinforced beams. For instance, Lestyowati et al. [23] reported that hybrid GFRP-reinforced concrete beams show approximately 28.77% less flexural strength than steel-reinforced beams. Regardless, GFRP's prime advantage of sustaining corrosion proves that it is still beneficial with minimal maintenance needed.

Additionally, it enhances the shear strength of the concrete structures, making shear failure less likely under loading conditions. Bui [17] stresses that the interfacial shear failure bond strength of GFRP with concrete influences shear behavior due to factors like the selection of adhesive and surface treatment aiding load transfer mechanisms. Other studies also showed that GFRP composites do not lose structural integrity under strongly damp conditions, thereby proving useful for marine and infrastructural works [24], [25]. It provides a sustainable

option for reinforcing concrete structures since it helps to avoid premature failures related to steel reinforcement, thus granting increased durability to the concrete structures.

In conclusion, the integration of GFRP plates in concrete beams represents a significant advancement in structural engineering, offering enhanced flexural and shear performance while improving durability in harsh environmental conditions. However, optimizing the bond strategies of GFRP remains fundamental to fully harnessing its application in the structure. Further investigation into the properties of adhesives, the behavior of bonds, and materials longevity is necessary to set proposed thresholds for standards of reinforced concrete structures with its reinforcements. Although it is significantly more costly than other used materials, its maintenance-free nature and corrosion-resistant qualities make it an economical solution in the long run. GFRP as a composite material aid to concrete structures is still under research and scrutiny; however, ACI Committee 440 [26] highlighted its potential and called for a wider investigation into its practicality within construction [27].

This study shows the bond strength, flexural capacity, and durability over time, which are some of the important attributes of GFRP-reinforced plain concrete beams. It helps understand the concealed performance elasticity that GFRP possesses, which allows evolving concrete infrastructures into stronger and more durable systems.

2. Methodology

This study aimed to assess the structural and bonding performance of concrete beam specimens that were strengthened with Glass Fibre Reinforced Polymer plates. Beam specimens with a cross-section of 100 mm x 100 mm x 500 mm were subjected to compressive strength tests and four-point bending tests.

2.1 Materials and Mix Preparation

As specified, the concrete mix included Type 1 Portland cement, fine aggregate, coarse aggregate, and water. The ratio was 1:1.93:3.43 by weight - that is, 1 part Type 1 Portland cement was replaced with 1.93 parts fine aggregate and 3.43 parts coarse aggregate with a ratio of 0.53 water to cement.

Concrete mixtures are essential for determining the properties of materials and modifying them to comply with specific requirements. It is possible to tailor mixes to individual needs by experimenting with different compatibility, cube compression, and slump tests. Changing the proportions of cement, water, and aggregate in concrete alters its properties, particularly its strength. The concrete mix design used throughout this study consists of 20.06 kg of cement, 10.83 kg of water, 38.76 kg of fine aggregate, and 68.86 kg of coarse aggregate. The concrete examples were made using a water-to-cement ratio of 0.53 and mix design per m³ as shown in Table 1. The sample production included vibrating the casting process, curing to ensure uniform strength, and cutting notches into the beams with saw-cutting table equipment.

Table 1 *The material and quantity used in the experiment*

Material	Quantity per m ³ (kg)
Cement	346
Water	187
Fine aggregate	668
Coarse Aggregate (10-20 mm)	1187
Water cement ratio	0.53

2.2 Slump Test

The practicability of the newly mixed concrete was assessed through observation by performing the slump test. Slump classes were determined in compliance with the standard by evaluating the consistency of samples and their stiffness in accordance with British Standard (BS) 8110 [28].

2.3 Compressive Strength Test

Tests for the concrete's compressive strength were carried out on prism specimens at 7, 14, 21, and 28 days after curing. While 7-day and 28-day strengths are common benchmarks, testing at 14 and 21 days provides a more detailed understanding of the strength development pattern of the concrete over time. This test measures the material's compressive stress and deformation in response to a compressive force, primarily to determine the compressive strength. While deformation was observed, the strain was not directly measured in these standard compressive strength tests. The focus was on determining the compressive strength according to ASTM

C39/C39M-20 [29]. Results are reported according to ASTM C39/C39M-20 [29], which include parameters like yield and ultimate strengths as well as elastic limit and modulus of elasticity.

2.4 Saw Cutting

After the curing process was complete, the beams were notched using a saw-cutting table machine. The concrete beam specimens were cut with the first notch. As illustrated in Fig. 1, these slots were placed centrally on the concrete beams. A steel saw was used to cut them close to the beam's midpoint after the concrete had hardened and dried. Notching was performed according to the Japanese Society of Civil Engineers (JSCE) Standard Specification for Concrete Structures (JSCE-SSCS) [30]. A saw-cut of 25 mm in depth and 2.5 mm in width was performed at the midspan of the prisms on the tension surface to guarantee flexure failure rather than shear. By separating the prism samples into a single bending zone, this saw-cut makes four-point bending testing easier. The saw-cut and increased shear span are designed to encourage flexural failure at the midspan rather than shear failure during the four-point bending test. It is important to note that shear forces are reduced, but not eliminated, within the beam.



Fig. 1 Notch made by saw cutting under the beam

2.5 Application of Epoxy

Abdullah et al. [16] stated that the best way to attach GFRP plates to concrete beams is by using Sikadur 31, as shown in Table 2. This method increases the beam's durability by 147% of the control beam's ultimate load. The 31-CF Sikadur Normal is a two-part thixotropic epoxy adhesive. The initial steps involve cutting the GFRP plate to the appropriate lengths. The GFRP plate is then dusted and polished to remove debris or impurities before installation. There is a 3:1 ratio between the white adhesive and black sticky components (Fig. 2). The plate and concrete surfaces are then coated with epoxy adhesive, and the GFRP plate is placed on top of the concrete. The prepared concrete surface was used to position the GFRP plate, and all air pockets were eradicated using a roller to ensure a strong bond between the epoxy and the concrete. Before testing the beam, the epoxy adhesive is allowed to cure for at least seven days.

Table 2 Composition and properties of Sikadur-31 epoxy adhesive

Property	Description/Value (Unit)
Composition	Epoxy resin
Appearance/Color	Part A: White paste; Part B: Dark grey paste; Mixed: Concrete grey
Density (Mixed)	1.90 ± 0.1 (kg/L)
Viscosity/Consistency	Thixotropic paste
Compressive Strength (7 days, +23°C)	~65 (N/mm ²)
Flexural Strength (7 days, +23°C)	~35 (N/mm ²)
Tensile Strength (7 days, +23°C)	~21 (N/mm ²)
Modulus of Elasticity in Compression (14 days, +23°C)	~4600 (N/mm ²)
Tensile Adhesion Strength (1 day, +10°C, Concrete Dry/Moist)	> 4 (N/mm ²)



Fig. 2 Plain concrete beam with GFRP plate (100mm x 200mm) bonded to the surface using Sikadur-31 epoxy

2.6 Flexural Test

The flexural test was carried out by positioning the 500 mm beam on two reaction stands and subjecting it to the four-point bending test. Each response stand had roller support installed to ensure it was readily sustained. The load was applied in the centre of the beam using a 500 kN hydraulic actuator that was mounted on a reaction frame. Based on the schematic diagram in Fig. 3, the hydraulic actuator's weight was distributed using two roller supports spaced 100 mm apart. A steel I-beam carried the weight from the hydraulic actuator to the roller supports. A Linear Variable Differential Transformer (LVDT) measured the mid-span deflection for every specimen.

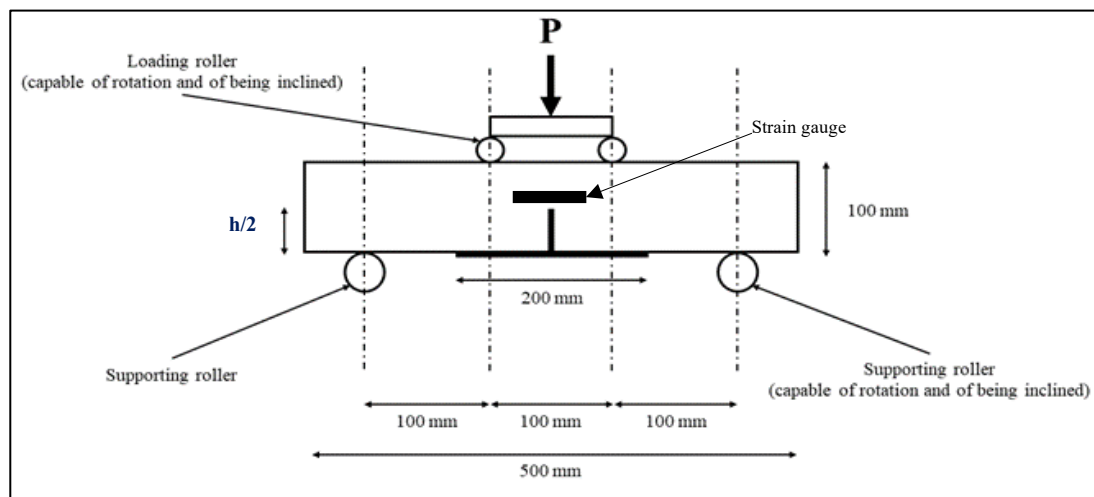


Fig. 3 Schematic diagram of four-point bending test as illustration

3. Results and Discussion

All testing, including slump tests, compressive strength tests, and four-point bending tests, were carried out at the concrete testing laboratory of UiTM Shah Alam Civil Engineering Faculty. This part describes in detail the evaluation and discussion of the experimental results. The workability of the fresh concrete mix was evaluated using slump tests. In contrast, the hardened concrete's compressive strength was empirically defined by means of cube tests over 28 days. Three concrete prisms with 100 mm x 100 mm cross-sections and 500 mm lengths were assessed for compressive strength at the age of 7, 14, 21, and 28 days of curing. The slump test is performed on the fresh concrete mix and has been shown to provide a measure of its consistency and workability. Usually, a lower slump value indicates a stiffer and less workable mix. In addition, four-point bending tests were carried out in order to determine the flexural strength characteristics of control beams and beams with GFRP plates of different sizes installed on them. In other words, the compressive strength test defines the ultimate compressive strength, which is the maximum compressive stress the concrete can sustain without failure. The next analysis will describe the remarkable increase in flexural strength, stiffness, and load-carrying capacity of the beams strengthened with GFRP compared to the other beams, especially when larger GFRP plates were used. The upcoming subsections will elaborate upon these findings and GFRP strengthening effectiveness, discussing the results in depth.

3.1 Workability Test Analysis

The workability of the new concrete mix was tested using slump tests shown in Table 3. A single batch of concrete was sampled and three slump tests were performed to provide a representative value for the measurement. The recorded slump results of the tests were 5.8 cm, 5.3 cm, and 5.6 cm. The concrete workability slump results of approximately 5.6 cm suggest satisfactory uniform workability achieved within the concrete batch. Moreover, all previously mentioned slump values were within the 3 to 6 cm value set by JKR guidelines, meaning that mix design is appropriate for the intended casting operations.

Table 3 Slump values from three slump tests on a single concrete batch

Slump test	Standard height of slump cone (cm)	Slump value (cm)
1	30	5.8
2	30	5.3
3	30	5.6

3.2 Compressive Strength Analysis

As a critical indicator of concrete grade, compressive strength is strongly associated with the hydration of the cement matrix. This research investigates the compressive strength achievements of concrete samples at 7, 14, 21, and 28 days of curing, profiling strength advancement over time. Evaluating compressive strength at different curing ages or intervals provides information about material durability and performance under load. As anticipated, the data collected illustrates ongoing strengthening in the concrete’s structure, characteristics typical of hydration hardening. The outcome of the compressive strength tests depicted in Table 4 confirms the existence of increasing strength, which is crucial to assessing the concrete’s withstand bearing value and the bonding in composite structures.

The average compressive strength values for the sample were observed at 39.19 MPa, 44.49 MPa, 46.75 MPa, and 49.08 MPa on days 7, 14, 21, and 28, respectively. Sample A was not factored into the computations for Day 21 owing to a defect-induced crack, which reduced the value to an anomalously low-stress level. Therefore, the average strength for Day 21 was calculated using Samples B and C only. Average compressive strength showed a 13.52% increase in lifting from 7 to 14 days, reaching a value of 44.49 MPa, as seen in Table 4. By Day 21, the value had increased further by approximately 5%, yielding 46.75 MPa. Following 28 days of water curing, the concrete reached its peak strength of 49.08 MPa, marking a final increase of 4.9%.

Improved bond strength between concrete and GFRP is achieved with elevated concrete compressive strength, thereby greatly multiplying the load-bearing capacity of composite structures. The strength evolution of the concrete mix is of paramount importance in assessing the flexural performance of GFRP-strengthened beams because compressive strength affects both structural behavior and bonding efficacy.

Table 4 Summary results of compressive strength

Sample	Day 7		Day 14		Day 21		Day 28	
	Max Load (kN)	Stress (MPa)	Max Load (kN)	Stress (MPa)	Max Load (kN)	Stress (MPa)	Max Load (kN)	Stress (MPa)
A	382.51	38.25	438.85	43.89	373.50	37.35	491.34	49.13
B	402.94	40.29	427.36	42.74	476.00	47.60	494.42	49.44
C	390.37	39.04	478.27	46.83	459.08	45.91	486.60	48.66
Average Strength (MPa)	39.19		44.49		46.75		49.08	

3.3 Flexural Analysis and Crack Pattern

The assessment of GFRP-strengthened components was carried out considering their flexural performance, evaluating the load-deflection response, propagation of cracks, shear stress, and failure mechanisms. Tests were performed according to ASTM D7958 standard for evaluation of the flexural reinforcement and bonding of GFRP

plates glued to the tension side of small notched beam samples. The results, as summarized in Table 5 and Fig. 4, show that the addition of GFRP plates considerably improved the load-bearing capacity and resistance to failure.

As noted in the four-point bending test, reinforcing the control beams with GFRP plates resulted in marked changes in behavior compared to the unstrengthened control beams. The control beams (CB) displayed an average ultimate load of 16.22 kN, with no strengthening or saw cuts and a flexural strength of 4.86 MPa. The deflection was 2.70 mm, and the strain was 1.02% prior to failure. These beams failed in a brittle manner, suddenly cracking at midspan followed by rapid fracture propagation towards the compression zone, leading to top fiber concrete crushing.

On the other hand, beams with 50 mm × 100 mm GFRP plates (GFRPP-50) achieved improvement in structural design and load-carrying capacity. The ultimate load for these beams improved to 24.83 kN, which is a 53% increase from the control beams, while flexural strength was 7.45 MPa. These additional specimens demonstrated slower crack propagation, lower crack openings, and more effective stress redistribution. The additional deflection of 2.93 mm and 1.10% strain indicated improved energy dissipation. Yet, unlike prior observations some variation in failure mechanisms was evident with GFRPP-50-2 shearing but GFRPP-50-1 and GFRPP-50-3 exhibiting a combined flexure-shear failure.

Additional structural improvements were documented in beams strengthened with 100 mm × 200 mm GFRP plates (GFRPP-100). The ultimate load for these soared to 38.56 kN, with control beams showing a 137% increase, making them the highest load-bearing specimens. Deflection increased to 3.00 mm, flexure strength peaked at 11.57 MPa, and strain climbed to 1.12%. This result achieved with the addition of large GFRP plates strengthens the claim that flexural resistance and ductility improve. However, the prominent failure modes of these specimens were shear and delamination failures, mainly in GFRPP-100-1 and GFRPP-100-3.

Table 5 Summary results of flexural test

Name of sample	Description	Load (kN)	Flexural Strength (kPa)	Deflection (mm)	Strain (%)
CB	<ul style="list-style-type: none"> No strengthening No saw cut 	16.22	4.86	2.7	1.02
GFRPP-50	<ul style="list-style-type: none"> Glass fiber reinforced polymer plate (50 mm × 100 mm) Saw cut 	24.83	7.45	2.93	1.10
GFRPP-100	<ul style="list-style-type: none"> Glass fiber reinforced polymer plate (100 mm × 200 mm) Saw cut 	38.56	11.57	3.00	1.12

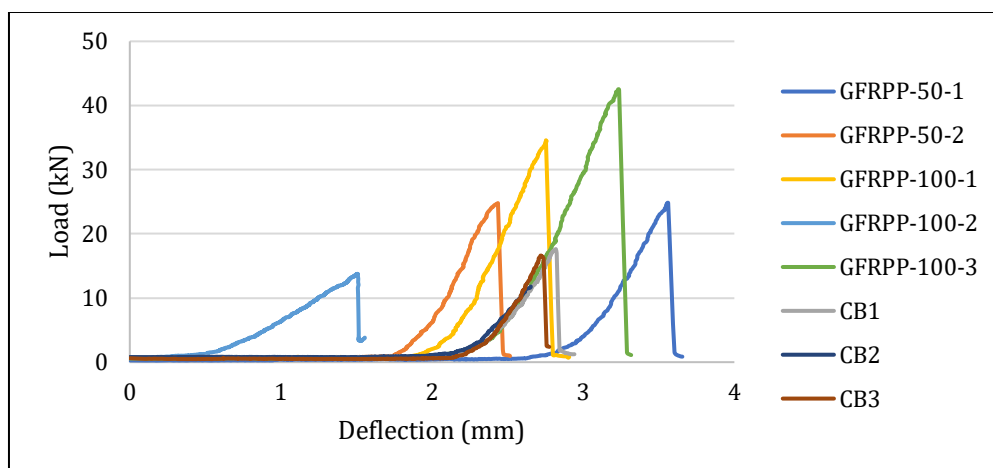


Fig. 4 Overall results of load against deflection for all types of plain beam specimens

The shear stress, ultimate load, and failure modes were obtained following the shear stress formula in Equation 1.

$$\tau = \frac{3PL}{5hwS} \quad (1)$$

where P = applied ultimate load (kN), L = specimen length (mm), h = specimen height (mm), w = composite sheet width (mm), and S = total composite sheet length (mm).

In Table 6, it can be observed that the greatest shear stress captured was 14.92 MPa, corresponding with GFRPP-50-1, which had an ultimate load of 24.83 kN, whereas the least was 2.06 MPa for GFRPP-100-2. The value of shear strength deviation varied to incorporate stress concentration, placement of the reinforcements, size of the reinforcements, and integration of the bond, thus becoming important for the structural engineering discipline. The considerations made about the placement of the epoxy glue and the surface treatment needed for the stress transfer are scientifically substantial. The application of inadequate adhesive leads to the phenomenon of brittle fracture at low-stress levels, which makes the case for improved prep work at the attachment points.

Table 6 Summary results of energy absorption and failure mode

Test specimen	Ultimate load, Pu (kN)	Shear stress, τ (Pa)	Failure mode
CB1	17.63	-	Flexure
CB2	14.41	-	Flexure
CB3	16.61	-	Flexure
Average	16.22	-	-
GFRPP-50-1	24.86	14.92	Flexure
GFRPP-50-2	24.79	14.87	Shear and debonding
GFRPP-50-3	15.94	9.56	Flexure
Average	24.83	14.90	-
GFRPP-100-1	34.58	5.19	Shear and delamination
GFRPP-100-2	13.76	2.06	Flexure
GFRPP-100-3	42.54	6.381	Shear and delamination
Average	38.56	5.78	-

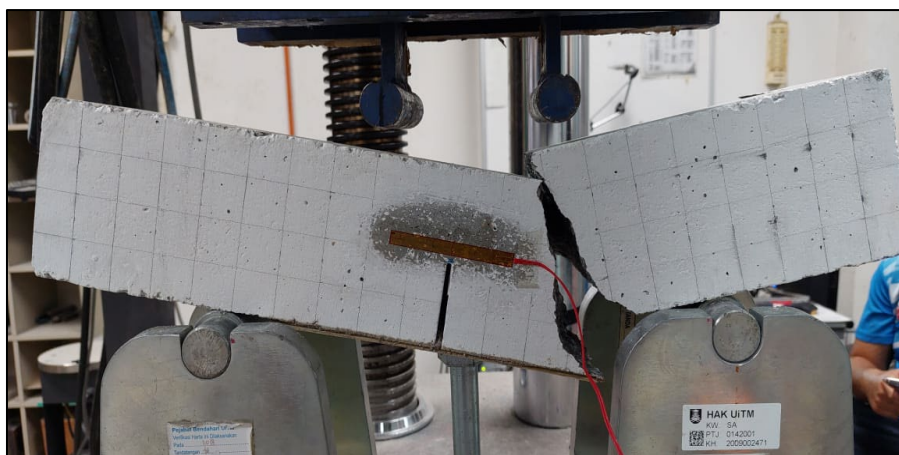


Fig. 5 Failure of sample GFRPP-100-3 after four-point bending test

The analysis of crack patterns shown in Fig. 5 suggests that GFRP strengthening had a marked positive effect on crack behavior. The control beams suffered sudden, wide cracking at midspan, which almost immediately advanced to the compression zone, culminating in rapid failure. On the other hand, beams with 50 mm × 100 mm GFRP plates showed smaller, more uniform cracks, which helped in mitigating strain concentration. Further increases in plate dimensions to 100 mm × 200 mm resulted in even better control of crack pattern formation. However, GFRPP-100 specimens did show indications of early disintegration failure, in contrast to the other specimens.

As was noted before, the GFRPP-100-3 specimen underwent a mixed Mode 4 shear and delamination failure post-four-point bending test. It emphasizes the importance of strong adhesive bonds between the GFRP and the concrete surface for optimal performance. Partial debonding by the GFRP plate leads to shear-induced pull-off of the reinforcement, which is known as edge delamination. These statements further validate the predominant role that the adhesive of the strengthening system plays by appreciating effective strengthening performance and its resultant structural integrity.

The outcomes are in agreement with the results of Hawileh et al. [31] study on the comparison of GFRP and CFRP laminates for flexural reinforcement. While CFRP laminates can bear greater ultimate loads and shear stresses, they also tend to debond due to adhesive failure prematurely. Hawileh's results showed that the laminates did improve load transfer efficiency, but the major drawback was the early failure in CFRP-reinforced beams. On the other hand, GFRP reinforcement is more economical and flexible, reducing the chances of sudden adhesive failure while significantly improving the structure. But to further increase the effectiveness of GFRP reinforcement, novel surface treatments and new formulations of epoxy resins need to be developed.

These results verify that the use of GFRP reinforcement enhances the load capacity, cracking, and energy absorption of concrete beams to a notable extent. The larger 100 mm × 200 mm GFRP plates showed the best structural performance. They contributed to enhanced ductility and better control of failure. However, the shear debonding failure observed reinforces the need to deal with bonding issues to avoid prematurely losing the backup cores.

The investigation in the future may highlight the issues related to the development of better epoxy bonding methods, examining the longitudinal behavior of GFRP plates under different environmental factors, and the application of hybrid reinforcement systems such as GFRP with CFRP for advanced structural stiffness. The remaining conclusions suggest that the use of GFRP plates for reinforcement enhances the strength and endurance of structures. However, additional efforts are needed to refine engineering practices to adapt them for construction use fully.

4. Conclusion

Incorporating GFRP plates as external reinforcement greatly improves the mechanical performance of concrete beams. Compared to the unrestrained specimens, the advanced beams exhibited substantial increases in load-bearing capacity, flexural strength, and resistance to cracking. Applying bigger GFRP plates proved to be even more effective for structural efficiency because they stiffer beams and delayed cracking. Failure analysis showed that advanced beams were better at controlling crack growth and absorbing energy. Some specimens, however, failed prematurely due to shear-induced debonding and delamination, which points to the critical role of bonding integrity. The results of the study demonstrate that GFRP reinforcement effectively changed the failure mechanisms of the beams, improving their durability and structural resilience. Proper adhesive bonding and the dimensions of the reinforcement greatly influenced optimizing performance, supporting the use of GFRP in strengthening concrete structures.

Acknowledgement

The authors would like to express their gratitude to the School of Civil Engineering and College of Engineering, Universiti Teknologi MARA, Shah Alam, for supporting this publication under grant Dana Dalaman Fakulti 600-TNCPI 5/3/DDF (KPK) (003/2023).

Conflict of Interest

Authors declare that there is no conflict of interests regarding the publication of the paper.

Author Contribution

The authors confirm contribution to the paper as follows: **study conception and design:** Sakhiah Abdul Kudus, Shahiron Shahidan; **data collection:** Nurul Ain Nafisa Kasmizi; **analysis and interpretation of results:** Ahmad Kamil Aminuddin, Nurul Ain Nafisa Kasmizi, Mohamad Farid Misnan; **draft manuscript preparation:** Ahmad Kamil Aminuddin, Sakhiah Abdul Kudus, Mohamad Farid Misnan, Sharifah Salwa Mohd Zuki, Shahiron Shahidan,

Mohamad Azim Mohammad Azmi, Nurul Ain Nafisa Kasmizi; All authors reviewed the results and approved the final version of the manuscript.

References

- [1] Kim, T.-K. & Park, J.-S. (2021) Performance Evaluation of Concrete Structures Using Crack Repair Methods, *Sustainability*, 13(6), 3217, <https://doi:10.3390/su13063217>
- [2] Navarro, I. J., Martí, J. V. & Yepes, V. (2019) Reliability-Based Maintenance Optimization of Corrosion Preventive Designs Under a Life Cycle Perspective, *Environmental Impact Assessment Review*, 74, 23-34, <https://doi:10.1016/j.eiar.2018.10.001>
- [3] Poursaee, A. (2016) *Corrosion of Steel in Concrete Structures*, Woodhead Publishing.
- [4] Gharieb, M., Elsayed, E. M., Abo-El-Enein, S. A., Sakr, K., Ali, A. & El-Sokkary, T. M. (2018) Influence of Some Industrial Wastes as a Heavy Aggregate on Durability of Concrete Upon Utilization in the Special Constructions, *Journal of Building Materials and Structures*, 5, 1-13. <https://doi:10.34118/jbms.v5i1.39>
- [5] Zhu, F., Ma, Z., & Zhao, T. (2016) Influence of Freeze-Thaw Damage on the Steel Corrosion and Bond-Slip Behavior in the Reinforced Concrete, *Advances in Materials Science and Engineering*, 9710678, 1-12, <https://doi:10.1155/2016/9710678>
- [6] Shamsad, Z. & Ahmad, S. (2017) *Durability of Concrete Structures: Investigation, Repair, Protection*. CRC Press.
- [7] Jiang, Z., Li, S., Fu, C., Zheng, D., Zhang, X., Jin, N. & Xia, T. (2021) Macrocell Corrosion of Steel in Concrete Under Carbonation, Internal Chloride Admixing and Accelerated Chloride Penetration Conditions, *Materials*, 14(24), <https://doi:10.3390/ma14247691>
- [8] Koulouris, K. & Apostolopoulos, C. (2020) An Experimental Study on Effects of Corrosion and Stirrups Spacing on Bond Behavior of Reinforced Concrete, *Metals*, 10(10), <https://doi:10.3390/met10101327>
- [9] Rushad, S. T. (2015) Experimental Investigations of RC Beams Strengthened With 4-Layerd Symmetric Cross-Ply (SCP) GFRP Laminates, *International Journal of Research in Engineering and Technology*, 4(13), 431-434, <https://doi:10.15623/ijret.2015.0425064>
- [10] Gooranorimi, O., Suaris, W., Dauer, E. A. & Nanni, A. (2017) Microstructural Investigation of Glass Fiber Reinforced Polymer Bars, *Composites Part B Engineering*, 110, 388-395, <https://doi.org/10.1016/j.compositesb.2016.11.029>
- [11] Pathak, P. & Zhang, Y. X. (2016) Finite Element Simulation for Nonlinear Finite Element Analysis of FRP Strengthened RC Beams with Bond-Slip Effect, *Applied Mechanics and Materials*, 846, 440-445, <https://doi:10.4028/www.scientific.net/amm.846.440>
- [12] Goldston, M., Remennikov, A. & Sheikh, M. N. (2016) Experimental Investigation of the Behaviour of Concrete Beams Reinforced with GFRP Bars Under Static and Impact Loading, *Engineering Structures*, 113, 220-232, <http://dx.doi.org/10.1016/j.engstruct.2016.01.044>
- [13] Kusnadi, K., Irmawaty, R. & Rauf, I. (2021) Deflection of Reinforced Concrete Beam CFRP Bar With U-Wrap CFRP Sheet as Shear Reinforcement, *E3S Web of Conferences*, 328, <https://doi:10.1051/e3sconf/202132810012>
- [14] Duo, Y., Liu, X., Liu, Y., Tafsirojjaman, T., & Sabbrojjaman, M. (2021) Environmental Impact on the Durability of FRP Reinforcing Bars, *Journal of Building Engineering*, 102909, <https://doi:10.1016/j.jobbe.2021.102909>
- [15] Emparanza, A. R., Caso Basalo, F. D., Kampmann, R., de Jalles, P. R. & Nanni, A. (2019) Durability of Mechanical Properties of GFRP Rebars Exposed to Seawater, *Construction and Building Materials*, 121492, <https://doi.org/10.1016/j.conbuildmat.2020.121492>
- [16] Abdullah, M. D., Abodi, J. T., & Ojaimi, M. F. (2022) Experimental behaviour of the reinforced concrete beams strengthened and repaired with steel plates, *Journal of Engineering Science and Technology*, 17(6), 3726-3741, https://jestec.taylors.edu.my/Vol%2017%20Issue%206%20December%202022/17_6_1.pdf
- [17] Bui, L. (2022) Effects of the bond properties of ETS-GFRP bar to concrete on the shear behavior of ETS-GFRP strengthened RC beams, *Structural Concrete*, 24(1), 1642-1655, <https://doi.org/10.1002/suco.202200026>
- [18] Rageh, B. O., El-Mandouh, M. A., Elmasry, A. H., & Attia, M. M. (2022) Flexural Behavior of RC Beams Strengthened with GFRP Laminate and Retrofitting with Novelty of Adhesive Material, *Buildings*, 12(9), <https://doi:10.3390/buildings12091444>

- [19] Zhong, Z., & Liu, H. (2017) Mode II Fracture of GFRP Laminates Bonded Interfaces Under 4-ENF Test, *Advances in Materials Science and Engineering*, 792346,1-10, <https://doi:10.1155/2017/3792346>
- [20] Yao, Y., Shi, P., Chen, M., Chen, G., Gao, C., Boisse, P. & Zhu, Y. (2022) Experimental and Numerical Study on Mode I and Mode II Interfacial Fracture Toughness of Co-Cured Steel-CFRP Hybrid Composites, *International Journal of Adhesion and Adhesives*, 112, <https://doi:10.1016/j.ijadhadh.2021.103030>
- [21] Yuan, J., & Hadi, M. N. S. (2017) Bond-Slip Behaviour Between GFRP I-Section and Concrete, *Composites Part B Engineering*, 130, 76-89, <https://doi:10.1016/j.compositesb.2017.07.060>
- [22] Xu, G., Yu, Y., Pan, Y. & Li, B. (2023) Durability of Bond Between Carbon/Glass Hybrid Fiber-Reinforced Polymer (HFRP) Bar and Concrete in Water, *Advances in Structural Engineering*, 26(9), <https://doi:10.1177/13694332231175391>
- [23] Lestyowati, Y., Herawati, H. & Panandita, B. S. (2023) Experimental Flexural Strength of Glass Fiber Reinforced Polymer (GFRP) Hybrid Reinforced Concrete Beams, *Jurnal Teknik Sipil*, 23(3), <https://doi:10.26418/jts.v23i3.67972>
- [24] Huang, J. & Davis, J. (2016) FE Evaluation of Reinforced Concrete Bridge Decks with Glass-FRP Composite Bars, *Key Engineering Materials*, 723, 776-781, <https://doi:10.4028/www.scientific.net/kem.723.776>
- [25] Wang, Z., Zhao, J., Liu, P., Zhang, X., Lu, Z. & Xie, J. (2024) Durability of Glass FRP Bar - reinforced Seawater-sea Sand Concrete Beams Under Sustained Loading in a Subtropical Coastal Environment, *Polymer Composites*, 283, <https://doi:10.1002/pc.28717>
- [26] ACI Committee 440 (2002) Guide for the Design and Construction of Externally Bonded FRP Systems for Strengthening Concrete Structures (ACI 440.2R-02), *American Concrete Institute*.
- [27] Khodadadi, N., Roghani, H., Harati, E., Mirdarsoltany, M., de Caso, F. R., & Nanni, A. (2024) Fiber-reinforced polymer (FRP) in concrete: A comprehensive survey, *Construction and Building Materials*, 432, 136634, <https://doi.org/10.1016/j.conbuildmat.2024.136634>
- [28] British Standards Institution (BSI). (1997) *BS 8110: Structural use of concrete*.
- [29] ASTM International. (2017) ASTM D7958/D7958M-17: Standard Test Method for Evaluation of Performance for FRP Composite Bonded to Concrete Substrate using Beam Test.
- [30] Japan Society of Civil Engineers (JSCE). (2007) Standard Specification for Concrete Structures (SCE-SSCS), *Japan Society of Civil Engineers*.
- [31] Hawileh, R., Al Nuaimi, N., Nawaz, W., Abdalla, J. & Sohail, M. (2022) Flexural and bond behavior of concrete beams strengthened with CFRP and galvanized steel mesh laminates, *Practice Periodical on Structural Design and Construction*, 27(1), [https://doi.org/10.1061/\(ASCE\)SC.1943-5576.0000651](https://doi.org/10.1061/(ASCE)SC.1943-5576.0000651)